

Measuring and Modeling of Multi-layered Subsurface Scattering for Human Skin

Tomohiro Mashita¹, Yasuhiro Mukaigawa², and Yasushi Yagi²

¹ Cybermedia Center Toyonaka Educational Research Center, Osaka University,
1-32 Machikaneyama, Toyonaka, Osaka 560-0043, Japan

² The Institute of Scientific and Industrial Research, Osaka University,
8-1 Mihogaoka, Ibaraki, Osaka 567-0047, Japan

mashita@ime.cmc.osaka-u.ac.jp, {mukaigaw,yagi}@am.sanken.osaka-u.ac.jp

Abstract. This paper introduces a Multi-Layered Subsurface Scattering (MLSSS) model to reproduce an existing human's skin in a virtual space. The MLSSS model consists of a three dimensional layer structure with each layer an aggregation of simple scattering particles. The MLSSS model expresses directionally dependent and inhomogeneous radiance distribution. We constructed a measurement system consisting of four projectors and one camera. The parameters of MLSSS were estimated using the measurement system and geometric and photometric analysis. Finally, we evaluated our method by comparing rendered images and real images.

1 Introduction

Dive into the Movie[1] is a system which, by scanning personal features such as the face, body shape, gait motion and so on, enables the members of an audience to appear in the movie as human characters. Technologies to reproduce a person in virtual space are important for these types of systems. In particular, good reproducibility of the skin is necessary for the further expression of personal features because it includes several aspects such as transparency, fineness, color, wrinkles, hairs, and so on.

Simulation of subsurface scattering is important for increasing the quality of the reproduced skin because some of the characteristics of the skin are the result of optical behavior under the skin's surface. Subsurface scattering is a phenomenon where light incident on a translucent material is reflected multiple times in the material and radiated to a point other than the incident point. If the transparency and inner components of the skin are expressed by simulating subsurface scattering, the expression of personal features will be improved.

Measurement and simulation of subsurface scattering are challenging problems. The Monte Carlo simulation method as typified by MCML [2] is one approach for subsurface scattering. This approach aims to simulate photon behavior based on physics and requires extravagant computational resources. When expressing complex media like human skin, it is also difficult to measure the parameters. Diffusion approximation [3] enables effective simulation of dense and

homogeneous media. However, there are limitations in the expression for reproducing human skin because this approximation ignores the direction of incident and outgoing light and assumes a homogeneous medium. Jensen et al. covered expressiveness using a combination of the single-scattering and dipole diffusion model [4]. Tariq et al. [5] expressed the inhomogeneity as Spatially Varying Sub-surface Scattering. They suggested that an inhomogeneous rendering method is important for the reproduction of real skin.

An expression of inhomogeneous scattering media and scattering dependent on the incoming and outgoing light direction is necessary to achieve a more expressive reproduction of real skin. The parameters of the scattering model must be measurable to reproduce real skin. In this paper we propose a Multi-Layered Subsurface Scattering model to achieve this requirement. We experimentally evaluated our system by comparing real images and images synthesized using the estimated parameters of the subsurface scattering.

Contribution

- The proposed model expresses a subsurface scattering model which is dependent on the direction of incoming and outgoing light. This **directional dependency** is achieved by the combination of simple scattering and a layered structure.
- The proposed model expresses an **inhomogeneous scattering** medium which is necessary for the reproduction of human skin including personal features.

Related Work

Rendering Method of Sub-Surface Scattering. Jensen proposed photon mapping [6] which traced individual photons for simulating volumetric subsurface scattering. Later, Jensen et al. proposed a dipole approximation [4] based on a diffusion approximation. Dipole approximation has been improved to a multipole model[7]. Ghosh et al.[8] proposed a practical method for modeling layered facial reflectance consisting of specular reflectance, single scattering and shallow and deep subsurface scattering. These methods were able to provide positive results for rendering photorealistic skin. The above methods are based on diffusion approximation. However, the importance of directional dependency is discussed. Donner et al. showed the disadvantage of diffusion approximation and proposed a spatially- and directionally-dependent model [9]. Mukaigawa et al. analyzed the anisotropic distribution of the lower-order scattering in 2D homogeneous scattering media [10].

Method for Measuring Subsurface Scattering. Various methods have been proposed for measuring subsurface scattering in translucent objects directly using a variety of lighting devices such as a point light source[11], a laser beam[4,12], a projector[5], and a fiber optic spectrometer[13].

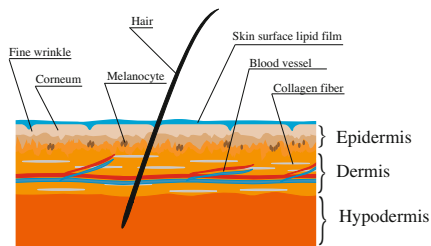


Fig. 1. Skin structure

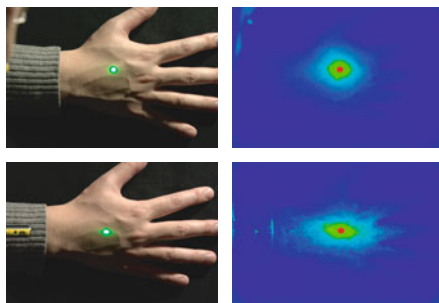


Fig. 2. SRD of a point illuminated hand

2 Expressing Spatial Radiance Distribution by Multi-Layered Subsurface Scattering

2.1 Spatial Radiance Distribution

Human skin has a complicated multi-layered structure and each layer consists of many components which have their own optical properties. The main components and skin structure are shown in Fig. 1. This complicated structure makes it difficult to render a photorealistic human face or skin and to measure the optical properties of the components of human skin. The structure of human skin is inhomogeneous in three dimensions. This inhomogeneity is reflected in the optical behavior of incident light. The inhomogeneity of optical behavior is observed as a Spatial Radiance Distribution (SRD) in the surface of the human skin.

Figure 2 shows the SRD in a hand by point illumination using a green laser pointer. Figure 2 left shows the experimental condition with general light. Figure 2 right shows the SRD with only the light of a laser pointer. In the upper row, laser light is incoming from the top of the hand. In the lower row, laser light is incoming from the left side of the hand. Obviously, the SRD in human skin is not homogeneous and depends on the direction of incoming light. We focus on the SRD and this paper describes the recreation of the SRD.

2.2 Concept of a Multi-Layered Subsurface Scattering Model

A simulation model to express the inhomogeneous and directionally dependent SRD is necessary for reproducing human skin. To reproduce a complicated SRD, an approximation model of the three-dimensional and inhomogeneous optical behavior is required. Furthermore, the parameters of the approximation model must be estimable. The important factor is not the number of parameters but the number of estimable parameters.

We propose the Multi-Layered Subsurface Scattering (MLSSS) model. The MLSSS model satisfies the above conditions when using a combination of the multi-layered structure and a simple scattering model. The three-dimensional

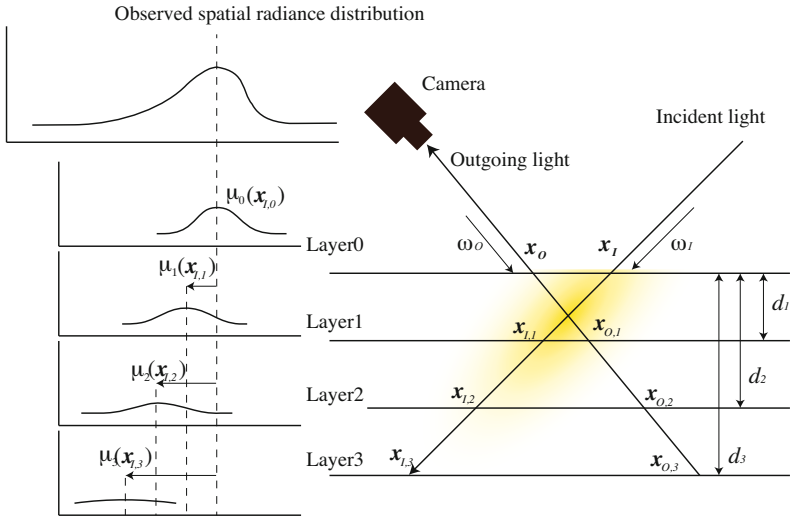


Fig. 3. Concept of MLSSS model

optical behavior is approximated by the layer structure. The observed SRD is expressed by a multiplication of the scattering in each layer. We define the scattering in each layer as simple isotropic scattering. Inhomogeneity of the SRD is expressed by each scattering particle having its own variables.

2.3 Details of the Multi-Layered Subsurface Scattering Model

The concept of this model is shown in Fig. 3. Figure 3 right shows incident light scattered by a translucent material, where the horizontal lines represent layers of the MLSSS model and arrows represent incident and outgoing light. The graph in the upper left shows the observed asymmetric SRD using the camera. The MLSSS model assumes that the asymmetric SRD is a mixture of simple distributions in each layer as shown in Fig. 3 left. The MLSSS model expresses a SRD that depends on the direction of the incident light and the viewpoint of the observer.

The Bidirectional Scattering Surface Reflectance Distribution Function (BSS-RDF) S expresses the relationship between incident radiance L_I and outgoing radiance L_O with incident and outgoing directions ω_I, ω_O and points $\mathbf{x}_I, \mathbf{x}_O$ as given in the following equation:

$$L_o(\mathbf{x}_O, \omega_O) = \int_{\Omega} \int_A S(\mathbf{x}_I, \omega_I; \mathbf{x}_O, \omega_O) L_I(\mathbf{x}_I, \omega_I) (\mathbf{n}(\mathbf{x}_I), \omega_I) d\omega_I dA(\mathbf{x}_I), \quad (1)$$

where Ω is a sphere, A is illuminated area, $\mathbf{n}(\mathbf{x}_I)$ is normal vector at the point \mathbf{x}_I , and ω_I, ω_O , and $\mathbf{n}(\mathbf{x}_I)$ are unit vectors. If an isotropic SRD is assumed, the direction of incoming and outgoing light can be ignored. The MLSSS model

proposed in this paper is an approximation of the BSSRDF but does not ignore the incoming and outgoing direction.

We assume incident radiance $L_I(\mathbf{x}_I, \boldsymbol{\omega}_I)$ at the point \mathbf{x}_I from the angle $\boldsymbol{\omega}_I$. In the MLSSS model, the observed point in each layer $\mathbf{x}_{O,l}$ shifts in proportion to the depth of the layer d_l , where l is layer number. The observed outgoing radiance L_O is expressed as

$$L_o(\mathbf{x}_O, \boldsymbol{\omega}_O) = \Sigma_l L_{O,l}(\mathbf{x}_{O,l}), \tag{2}$$

where

$$\mathbf{x}_{O,l} = \mathbf{x}_O + \frac{d_l}{(\mathbf{n}, \boldsymbol{\omega}_O)} \boldsymbol{\omega}_O. \tag{3}$$

Thus the dependence on the outgoing direction of the MLSSS is defined.

The SRD in each layer is assumed to be an isotropic distribution and independent of the direction of incident light similar to the diffusion approximation. The BSSRDF function in each layer is expressed as $D(\mathbf{x}_O, \mathbf{x}_I)$, where \mathbf{x}_I is the incident point. Thus the relationship between the incident and outgoing radiance in each layer is

$$L_{O,l} = D(\mathbf{x}_{O,l}, \mathbf{x}_{I,l})(\mathbf{n}(\mathbf{x}_I), \boldsymbol{\omega}_I) L_{I,l}, \tag{4}$$

where $\boldsymbol{\omega}_I$ is the direction of the incoming light, $\mathbf{n}(\mathbf{x}_I)$ is the normal vector at \mathbf{x}_I , $L_{I,l}$ is a part of the incident light scattered in layer l .

The incident point in each layer also shifts in proportion to the depth of the layer d_l . The incident point in a layer $\mathbf{x}_{I,l}$ is obtained from the following equation:

$$\mathbf{x}_{I,l} = \mathbf{x}_I + \frac{d_l}{(\mathbf{n}, \boldsymbol{\omega}_I)} \boldsymbol{\omega}_I. \tag{5}$$

$L_{I,l}$ is obtained by

$$L_{I,l} = \frac{w_l}{w_a + \Sigma_l w_l} L_I, \tag{6}$$

where w_l is the weight of light scattered in the layer l and w_a is the weight of absorbed light.

Finally, the relationship between the outgoing radiance $L_O(\mathbf{x}_O, \boldsymbol{\omega}_O)$ and the incident radiance $L_I(\mathbf{x}_I, \boldsymbol{\omega})$ is expressed as

$$L_O(\mathbf{x}_O, \boldsymbol{\omega}_O) = \Sigma_l D(\mathbf{x}_{O,l}, \mathbf{x}_{I,l})(\mathbf{n}(\mathbf{x}_I), \boldsymbol{\omega}_I) L_I(\mathbf{x}_I, \boldsymbol{\omega}). \tag{7}$$

The case of general lighting is expressed as

$$L_O(\mathbf{x}_O, \boldsymbol{\omega}_O) = \int_{\Omega} \int_A \Sigma_l D(\mathbf{x}_{O,l}, \mathbf{x}_{I,l})(\mathbf{n}(\mathbf{x}_I), \boldsymbol{\omega}_I) L_I(\mathbf{x}_I, \boldsymbol{\omega}) d\boldsymbol{\omega} dA(\mathbf{x}_I). \tag{8}$$

The BSSRDF function in the MLSSS model is

$$S(\mathbf{x}_I, \boldsymbol{\omega}_I; \mathbf{x}_O, \boldsymbol{\omega}_O) = \Sigma_l D(\mathbf{x}_{O,l}, \mathbf{x}_{I,l})(\mathbf{n}(\mathbf{x}_I), \boldsymbol{\omega}_I) \frac{w_l}{w_a + \Sigma_l w_l}. \tag{9}$$

This BSSRDF function retains the dependence on direction and consists of isotropic scattering, layer distance, and weight parameters.

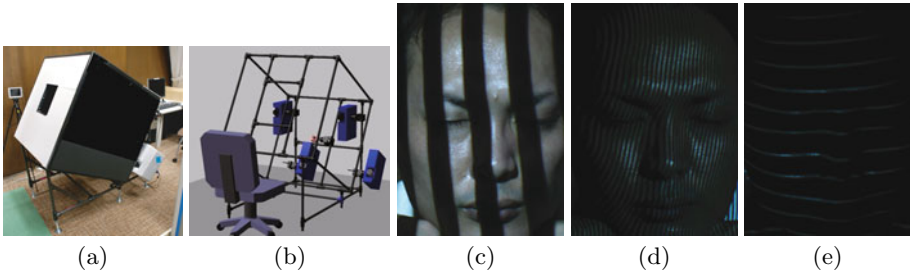


Fig. 4. MLSSS measurement system ((a) Hardware and (b) Configuration of camera and projectors) and Samples of captured images ((c) Structured light, (d) High frequency, (e) Line sweeping)

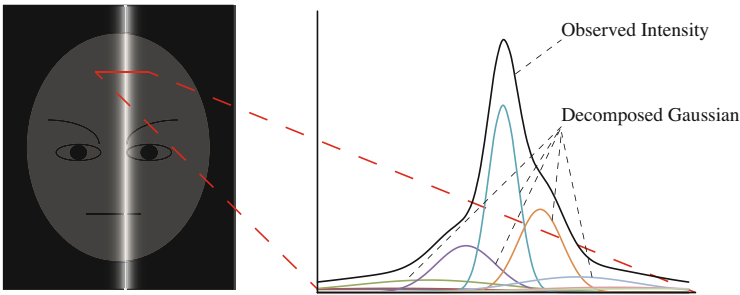


Fig. 5. Schematic diagram of parameter estimation

3 Measuring System

3.1 Hardware

We have constructed an implement for capturing facial images with pattern projection and a system for parameter estimation by geometric and photometric analysis.

The measurement system is shown in Fig. 4(a) and (b). The measurement system consists of 4 LCD projectors and a camera. The inside of the measurement system is a black box with a hole for inserting a face and 4 holes for the projectors. The size of the box is $90\text{cm} \times 90\text{cm} \times 90\text{cm}$. The camera is a Lw160c (Lumenera) with 1392×1042 pixel and 12 bit valid data for each pixel. The projectors are EMP-X5 (EPSON) with 1024×768 pixel and 2200 lm. The positions of the camera and projectors are shown in Fig. 4(b).

3.2 Geometric and Photometric Analysis

We describe the parameter estimation for the MLSSS model. The geometric parameters estimated are ω_O , ω_I , \mathbf{n} , and the shape of a face. The photometric

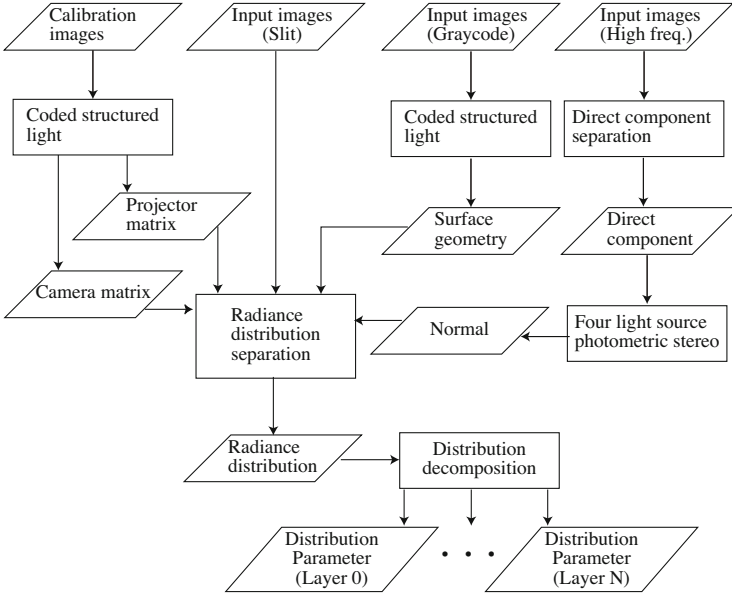


Fig. 6. Geometric photometric analysis

parameters estimated are the σ and w_l included in the scattering particles because we use Gaussian distribution, $D(\cdot)$. Figure 6 shows the flow of the geometric and photometric analysis.

A structured light, slit pattern and high-frequency pattern are projected from each projector. Figures 4(c), (d), and (e) show samples of captured images with projected patterns. The shape of the face is reconstructed using the coded structured light projection method [14]. The captured images with high-frequency patterns are used for direct component separation [15]. The separated direct components are used for the normal vector estimation using the four light source photometric stereo method [16].

We extracted a one dimensional SRD from this geometric information and the slit line projected images. We took this one dimensional radiance distribution as a distribution mixture of the simple radiance distributions in each layer. Figure 5 shows a schematic diagram of the photometric parameter estimations. Scattering parameters are estimated by an EM algorithm.

4 Experiments

We conducted experiments to evaluate our model and measuring system by rendering. The conditions of rendering are as follows. The camera position was fixed and the same as when the image was captured. The light position was not the same as when the image was captured. To evaluate the MLSSS model, we

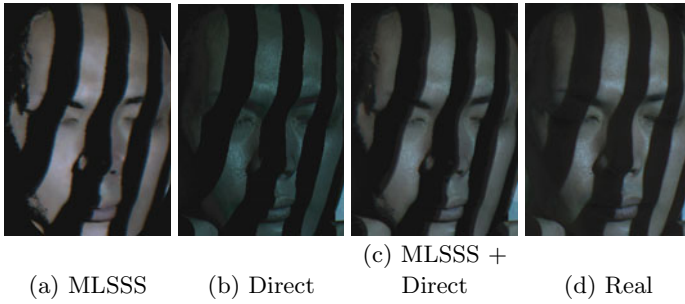


Fig. 7. Synthesized image with stripe projection

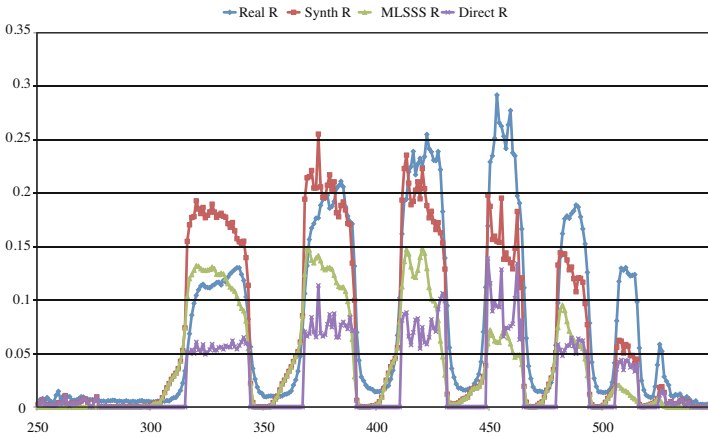


Fig. 8. A profile of Fig. 7 of red plane and $y = 150$

used captured images with three light sources for parameter estimation and the remaining unused images were used for comparison with the rendered images. We rendered the image of a face with the camera and a light position identical to when the image was captured. The mixture distribution was decomposed by an EM algorithm, with 20 mixtures.

4.1 Evaluation of Anisotropic Scattering

We rendered an image with a strip light to evaluate the expression for anisotropic scattering. Figure 7(a) shows the rendered subsurface scattering. Figure 7(b) shows the separated direct component of a real image. Figure 7(c) shows the sum of Fig. 7 (a) and Fig. 7(b). Figure 7 (d) shows a real image with the same lighting conditions as the rendered image. We can compare Fig. 7(c) to Fig. 7(d) and it is obvious that the rendered subsurface scattering using the MLSSS model enables a reproduction of the directionally dependent subsurface scattering.

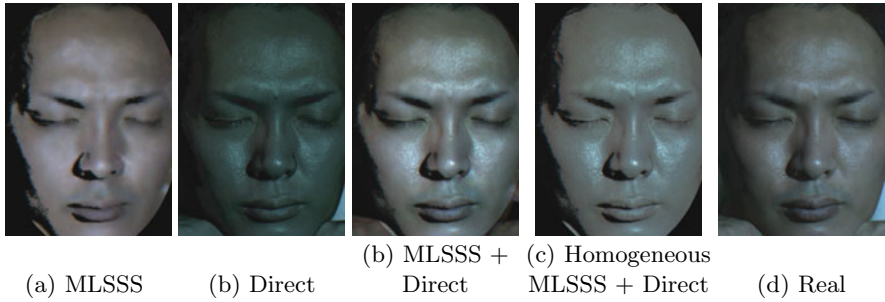


Fig. 9. Rendered image with point light source

The red color's profile from left to right of the image is shown in Fig. 8. In Fig. 8, the position of the light source is on the right side. The pixels with low values are not illuminated. We can see the effect of subsurface scattering from the boundaries between the illuminated and non-illuminated area. There are differences in the illuminated area's intensity between the Real and Synthesized images. We think that the parameters of subsurface scattering include the influence of the position of the light source.

4.2 Evaluation of Inhomogeneity

We rendered an image of subsurface scattering with a point light source to evaluate the expression of inhomogeneity. Figure 9 shows the result of rendering with a point light source. Figure 9(a) is a synthesized indirect component using the MLSSS model. Figure 9(b) is the direct component of the real image. Figure 9(c) is Fig. 9(b) + Fig. 9(c). Figure 9(d) is rendered using the same parameters for all the scattering particles in each layer. The parameters for Fig. 9(d) are the mean of each parameter. Figure. 9(e) is a real image with the same light source for comparison. We can see the blood vessels, facial hair roots, and inhomogeneous redness in Fig. 9(a) and Fig. 9(c). However, we cannot see the components of the inside of the skin from Fig. 9(c). It is obvious that the inhomogeneity of subsurface scattering is important for the reality of rendered skin. However, the direct component is also important to express the texture of real skin.

5 Conclusions

In this paper, we proposed the MLSSS model. This model expresses the SRD of the surface of translucent material depending on the direction of the incident and outgoing light. The MLSSS model has pixel-level variation of the scattering parameters. We constructed a measurement system consisting of a camera and four projectors. The parameters of the MLSSS model are estimated from the captured images by geometric photometric analysis. In the experiments, images of subsurface scattering are rendered and compared with real images. Future work includes investigating other scattering models and layer structures.

References

1. Morishima, S.: Dive into the Movie -Audience-driven Immersive Experience in the Story. *IEICE Trans. Information and Systems* E91-D(6), 1594–1603 (2008)
2. Wang, L., Jacques, S.L., Zheng, L.: Monte carlo modeling of light transport in multi-layered tissues. *Computer Methods and Programs in Biomedicine* 47(2), 131–146 (1995)
3. Stam, J.: Multiple scattering as a Diffusion Process. In: *Eurographics Workshop in Rendering Techniques 1995*, pp. 51–58 (1995)
4. Jensen, H.W., Marschner, S.R., Levoy, M., Hanrahan, P.: A practical model for subsurface light transport. In: *SIGGRAPH 2001*, pp. 511–518 (2001)
5. Tariq, S., Gardner, A., Llamas, I., Jones, A., Debevec, P., Turk, G.: Efficient estimation of spatially varying subsurface scattering parameters. In: *VMV 2006*, pp. 165–174 (2006)
6. Jensen, H.W.: *Realistic Image Synthesis using Photon Mapping*. AK Peters, Wellesley (2001)
7. Donner, C., Jensen, H.W.: Light diffusion in multi-layered translucent materials. In: *SIGGRAPH 2005*, pp. 1032–1039 (2005)
8. Ghosh, A., Hawkins, T., Peers, P., Frederiksen, S., Debevec, P.E.: Practical modeling and acquisition of layered facial reflectance. In: *SIGGRAPH Asia 2008* (2008)
9. Donner, C., Lawrence, J., Ramamoothi, R., Hachisuka, T., Jensen, H.W., Nayar, S.K.: An Empirical BSSRDF Model. In: *SIGGRAPH 2009* (2009)
10. Mukaigawa, Y., Yagi, Y., Raskar, R.: Analysis of Light Transport in Scattering Media. In: *CVPR* (2010)
11. Mukaigawa, Y., Suzuki, K., Yagi, Y.: Analysis of subsurface scattering under generic illumination. In: *ICPR 2008* (2008)
12. Goesele, M., Lensch, H.P.A., Lang, J., Fuchs, C., Seidel, H.P.: Disco - acquisition of translucent objects. In: *SIGGRAPH 2004*, pp. 835–844 (2004)
13. Weyrich, T., Matusik, W., Pfister, H., Bickel, B., Donner, C., Tu, C., McAndless, J., Lee, J., Ngan, A., Jensen, H.W., Gross, M.: Analysis of human faces using a measurement-based skin reflectance model. In: *SIGGRAPH 2006*, pp. 1013–1024 (2006)
14. Inokuchi, S., Sato, K., Matsuda, F.: Range imaging system for 3-D object recognition. In: *ICPR*, pp. 806–808 (1984)
15. Nayar, S.K., Krishnan, G., Grossberg, M.D., Raskar, R.: Fast separation of direct and global components of a scene using high frequency illumination. In: *SIGGRAPH 2006*, pp. 935–944 (2006)
16. Barsky, S., Petrou, M.: The 4-source photometric stereo technique for three-dimensional surfaces in the presence of highlights and shadows. *IEEE Transactions on Pattern Analysis and Machine Intelligence* 25(10), 1239–1252 (2003)